

# Plastic zone size measurement with synchrotron radiation

Y. Prawoto\*, R.A. Winholtz\*<sup>†</sup>, D.R. Haeffner<sup>▲</sup>, and P.L. Lee<sup>▲</sup>

\*Department of Mechanical and Aerospace Engineering, University of Missouri, Columbia, MO 65211 USA

<sup>†</sup>Research Reactor Center, University of Missouri, Columbia, MO 65211 USA

<sup>▲</sup>Advanced Photon Source, Argonne National Laboratory, Argonne, IL 60439 USA

## Introduction

Changes in the plastic zone size determined with diffraction line broadening are used to verify an analysis of the maximum stress intensity factor (SIF) for a fatigue crack grown in a tensile residual stress field.

## Methods and Materials

### Sample and fatigue testing

An ASTM-type CT specimen [1], shown in Figure 1, of 1080 steel was used. The steel was spheroidized by heating at 800° C for 30 minutes, quenching with and then tempering at 800° C for 3 hours. The ferrite grain size was approximately 5.6 μm, while the cementite particles had an average size of 1 μm. Residual stresses were introduced by hydraulically pressing an oversized tapered pin into a tapered hole. A companion specimen without the tapered hole and interference pin was used for comparison.

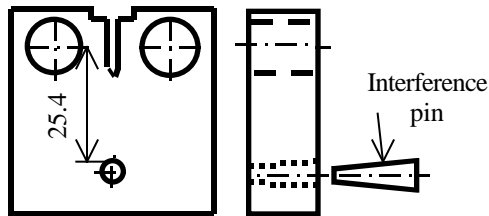


Figure 1: CT specimen with interference pin.

The cracks were grown with a constant applied SIF range of 25 MPa m and an applied load ratio of 0.1. The crack length was measured using the compliance method [1].

### Initial residual stress measurements

The initial residual stresses were measured using x-ray diffraction at Northwestern University [2]. Chromium characteristic x-rays of wavelength 2.2897 Å were used with a spot size of 210 μm on the surface of the specimen.

### Plastic zone measurement

The specimen was sectioned perpendicular to the crack plane with a water-cooled abrasive wheel. This gave experimental access to an interior plane of the specimen. To eliminate the material damage introduced during the cutting process, the interior surface was metallographically polished and etched. Final polishing was done with 0.05 μm alumina powder and etching was done with 2% nital.

The plastic zone around the crack was examined by using diffraction peak broadening to reveal material that had experienced plastic deformation. The experiments were conducted using synchrotron radiation from the SRI-CAT

beamline 1-BM at the Advanced Photon Source at Argonne National Laboratory. A focused 10 keV x-ray beam was used with a spot size of 50 x 50 μm produced at the specimen position by use of crossed tungsten slits. The specimen was mounted on a translator that allowed orthogonal motions perpendicular to the x-ray beam with 1 μm resolution. The ferrite 411 diffraction peak at approximately 133° 2θ was observed for line broadening.

The experiment started with finding the position of the crack surface in relation to the x-ray beam. The position of the crack face in relation to the beam was found for each crack length investigated by monitoring the fluorescence produced by the specimen as the crack face was scanned across the beam. The position where the iron fluorescence reached half its full value was recorded as the crack face for that particular crack length.

Once the crack face was found, diffraction peaks were recorded at a series of distances from the crack face. Near the crack face the diffraction peaks were broadened from plastic deformation. The diffraction peaks were fit to a Gaussian function with a linear background to determine their full width at half maximum (FWHM). The location where the FWHM returned to its value remote from the crack face was then defined as the boundary of plastic zone.

## Results

### Fatigue crack propagation

The fatigue crack propagation rate was accelerated significantly compared to that in a sample with no initial residual stress, which has a constant propagation rate.

### Residual stresses and the plastic zone

Figure 2 shows the initial residual stress distribution before fatigue cracking. Finite element modeling of the insertion process gives comparable results for the faces and shows that the stress distribution in the interior is similar [3]. The residual stresses were then converted to a residual SIF using the weight function,  $m(a,x)$ , for a CT specimen and the relation [4, 5, 6]

$$K_R = \int_0^a (x) \gamma m(a,x) dx \quad (1)$$

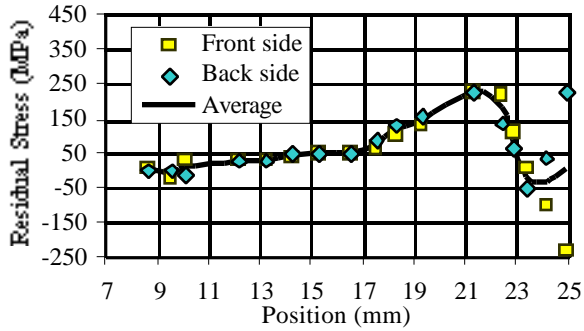


Figure 2: Initial residual stress along prospective crack line.

Figure 3 shows the residual SIF versus crack length calculated using Equation 1.

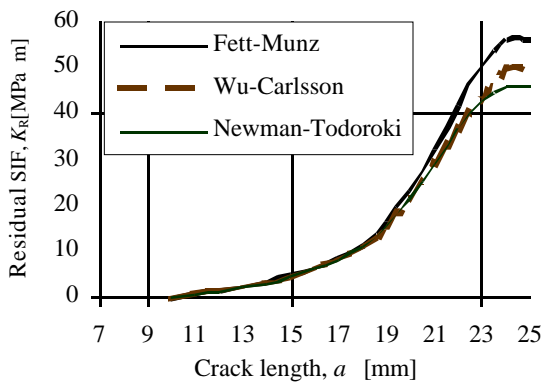


Figure 3: Residual stress intensity factors calculated using three different weight function solutions.

Figure 4 shows the height of the plastic zone as measured for points along the crack length. The data show that as the crack grows into the tensile residual stresses the plastic zone size increases.

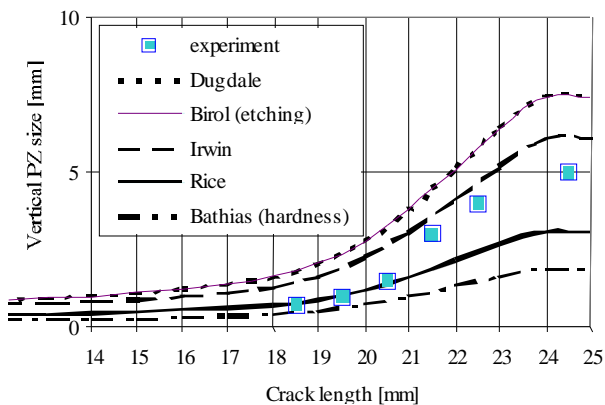


Figure 4: Vertical plastic zone size compared with results of different theories and experiments [7-10].

## Discussion

It is convenient to use a linear elastic fracture mechanics approach, because once the stresses have been converted to SIF, addition can be easily performed with the superposition principle. For a specimen without residual stresses, the maximum SIF is the same for all crack lengths,

$$K_{\max} = \frac{K}{(1-R)} \quad (2)$$

For the constant applied SIF range  $K=25 \text{ MPa m}$  and a load ratio  $R=0.1$ ,  $K_{\max}$  is  $27.78 \text{ MPa m}$ . On the other hand, for a sample containing residual stresses, the residual SIF should be added based on the superposition principle,

$$K_{\max} = K_R + \frac{K}{(1-R)} \quad (3)$$

The first term of the right side,  $K_R$ , is the residual SIF shown in Figure 4, while the second term remains  $27.78 \text{ MPa m}$ . Thus, as the crack grows and sees a larger residual SIF,  $K_{\max}$  will increase resulting in a larger plastic zone.

In Figure 4, the experimental results are compared with calculated plastic zone sizes using Equation 3 and several constants obtained analytically and experimentally [7-10]. The experimental constants vary because they are obtained by different methods with different criteria for the boundary of the plastic zone. The experimental data obtained through diffraction line broadening falls between Irwin's and Rice's analytical solutions, which are upper and lower bounds. The figures also show that Birol's method predicts higher plastic zone sizes because, it can be assumed, the etching method has a higher resolution for plastic deformation for the material that he used. On the other hand, the microhardness method predicts lower plastic zone sizes. This implies that the microhardness method has a lower sensitivity to plastic deformation.

## Acknowledgments

This work was supported by the University of Missouri Research Board. The use of the Advanced Photon Source was supported by the U.S. Department of Energy, Basic Energy Sciences, Office of Science, under Contract No. W-31-109-Eng-38. The authors also gratefully acknowledge J.D. Almer for providing the initial residual stress measurements.

## References

- [1] ASTM Designation E 647-95a, (American Society for Testing and Materials, Philadelphia, PA, 1995) 565-601.
- [2] J.D. Almer, *Met. and Matls. Trans.* **29A**, 2127-2136 (1998).
- [3] J.D. Almer, J.B. Cohen, K.R. McCallum, and R.A. Winholtz, *Proc of 5<sup>th</sup> ICRS, Bethel, CT*, 1072-1077 (1997).
- [4] A. Todoroki and H. Kobayashi, *Trans. of the Japan Soc. of Mech. Eng.* **A54**, 30-36 (1988).
- [5] X.R. Wu and A.J. Carlsson, *Weight functions and stress intensity factor solutions*, (Pergamon Press, Oxford, UK, 1991).

- [6] T. Fett and D. Munz, *Stress Intensity Factors and Weight Functions*, (Comp. mech publication, Southampton, UK, 1997).
- [7] D.S. Dugdale, *J. Mech. Phys. Solids*, **8**, 100–108 (1960).
- [8] G.R. Irwin, *Proc of 7<sup>th</sup>. Sagamore Ordnance Materials Conference, Syracuse University* **IV**, 63–78 (1960).
- [9] C. Bathias and R.M. Pelloux, *Metall. Trans.* **4**, 1265–1273 (1973).
- [10] Y. Birol, *J. Mater. Sci.* **23**, 2079–2086 (1988).